**ROYAL AERONAUTICAL SOCIETY**

**RESEARCH ARTICLE**

# Modeling and analysis of nonlinear dynamics of axisymmetric vector nozzle based on deep neural network

X. Wang[1,2,3,*] , H. Hu[1,*] , Z. Chen[1], H. Wang[1], L. Ye[3] and G. Ye[3]

[1]School of Mechanical Engineering and Automation, Northeastern University, Shenyang, China
[2]Key Laboratory of Vibration and Control of Aero-Propulsion System, Ministry of Education, Northeastern University, Shenyang, PR China
[3]AECC Shenyang Engine Research Institute, Shenyang, China
**Corresponding author:** X. Wang; Email: wangxy@me.neu.edu.cn

**Abstract**
The axisymmetric nozzle mechanism is the core part for thrust vectoring of aero engine, which contains complex rigid-flexible coupled multibody system with joints clearance and significantly reduces the efficiency in modeling and calculation, therefore the kinematics and dynamics analysis of axisymmetric vectoring nozzle mechanism based on deep neural network is proposed. The deep neural network model of the axisymmetric vector nozzle is established according to the limited training data from the physical dynamic model and then used to predict the kinematics and dynamics response of the axisymmetric vector nozzle. This study analyses the effects of joint clearance on the kinematics and dynamics of the axisymmetric vector nozzle mechanism by a data-driven model. It is found that the angular acceleration of the expanding blade and the driving force are mostly affected by joint clearance followed by the angle, angular velocity and position of the expanding blade. Larger joint clearance results in more pronounced fluctuations of the dynamic response of the mechanism, which is due to the greater relative velocity and contact force between the bushing and the pin. Since axisymmetric vector nozzles are highly complex nonlinear systems, traditional numerical methods of dynamics are extremely time-consuming. Our work indicates that the data-driven approach greatly reduces the computational cost while maintaining accuracy, and can be used for rapid evaluation and iterative computation of complex multibody dynamics of engine nozzle mechanism.

## Nomenclature

| | |
|---|---|
| DNN | Deep Neural Network |
| ROM | Reduced Order Model |
| ReLU | Rectified Linear Unit |
| Adam | Adaptive Moment Estimation |
| MAE | Mean Absolute Error |
| MSE | Mean Squared Error |
| RMSE | Root Mean Squared Error |

## 1.0 Introduction

Vector nozzle technology can improve the short takeoff and landing capability [1], and promote the manoeuvering agility of fighter aircraft [2]. The axisymmetric vector nozzle is one of the main types of vector nozzles [4]. It consists of complex multistage connecting rods with flexible components and a

---

*These two authors contributed equally to this work.

large number of joint clearances [31]. These factors can lead to changes in the kinematic characteristics and driving force of the nozzle mechanism, affecting the stability of its operation [9], and pose significant challenges for the rapid modeling and evaluation of nozzle mechanism performance [10].

Various external factors such as machining, assembly errors and wear errors produce different sizes of joint clearance, which will significantly affect the motion accuracy and dynamic response of the axisymmetric vector nozzle [32]. By establishing a deep neural network (DNN) model of the axisymmetric vector nozzle, the effect of joint clearance parameters on the kinematic and dynamic characteristics of the mechanism can be efficiently investigated [33]. The dynamic response of the nozzle mechanism is sensitive to the variation of the joint clearance parameters. Therefore, it is necessary to study the effect of joint clearance on the dynamic response for axisymmetric vector nozzle mechanisms with high accuracy requirements.

Machine learning and agent models are used to study the dynamic problems of vehicles, robots and railroads or to identify nonlinear control parameters [11], but very little research has been done in the field of aero-engine adjusting mechanisms. Kraft et al. used a black box modeling approach to simulate multibody dynamics of vehicle system, estimate the track geometry and analyse vehicle response to measured trajectories [16]. Ansari et al. established a neural network-based nonlinear tire model to simulate the dynamic response of a real tire, and speed up the calculation of the dynamic response of the vehicle model [14]. Yu et al. proposed a DNN-based simulation model for rail vehicles to predict the acceleration response of axle boxes corresponding to different dimensions and vehicle speeds [25]. Kurvinen et al. used a data-driven modeling approach to accelerate the design process and provide efficient models to address control challenges. Neural networks are able to solve multibody dynamics problems and predict the response quickly and reliably [20, 22], provide strong means to identify nonlinear parameters in the control equations or estimating multibody dynamics in a probabilistic sense [17, 19]. Go et al. proposed that a date driven based reduced order model (ROM) can effectively improve the simulation efficiency of multibody dynamics [12]. Ting et al. attempted to apply Bayesian networks in multibody dynamics simulations, which were able to automatically detect relevant features of the model and reduce the effect of noise on the model [23, 24]. The above research papers show that the application of machine learning in multibody dynamics systems achieves excellent results. DNN is chosen in this paper because it offers significant advantages over other surrogate models like kriging [3]. For example, DNN has strong expressive power and flexibility, can handle complex nonlinear relationships, and automatically extract features, making them suitable for high-dimensional and large-scale problems [6]. The accuracy and effectiveness of DNN in the multibody dynamics field have been validated, and the axisymmetric vector nozzle is a typical multibody dynamics system, therefore DNN is selected as the surrogate model for analysing axisymmetric vector nozzles.

The axisymmetric vector nozzle mechanism is a typical multibody dynamics system [8], and considering the cited literature on the application of machine learning in multibody dynamics systems, the data-driven approach based on DNN is expected to build highly accurate and low-cost agent models for the axisymmetric vector nozzle mechanism. The development of machine learning provides a valuable opportunity for efficiently and accurately designing and analysing axisymmetric vector nozzles.

The axisymmetric vector nozzle mechanism is a typical multibody dynamics system. In recent years, machine learning has been extensively researched within the field of multibody dynamics. This study verifies the feasibility of using machine learning for multibody dynamics analysis. Furthermore, it offers the possibility of employing DNN to simulate the axisymmetric vector nozzle mechanism. Considering the complex structure and strong nonlinearity of the axisymmetric vector nozzle, a well-trained DNN is built to analyse the kinematics and dynamics of the axisymmetric vector nozzle system. The effect of the joint clearance on the dynamic response of the axisymmetric vector nozzle is investigated. DNN is proved to be an effective model capable of predicting the dynamic response of axisymmetric vector nozzles with high accuracy, low cost and high efficiency.
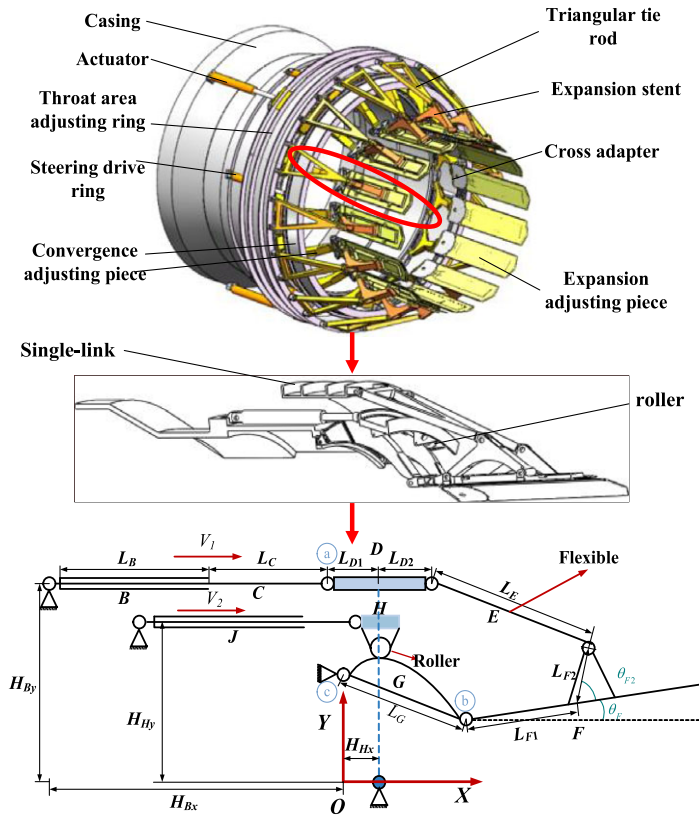
**Figure 1.** *Axisymmetric vector nozzle modeling diagram.*

## 2.0 Multibody dynamics modeling approach

### 2.1 The dynamic equations for the axisymmetric vector nozzle mechanism

A typical axisymmetric vector nozzle mechanism mainly contains: casing, actuator, throat area adjusting ring, steering drive ring, tie rods, convergence adjusting piece and expansion adjusting piece [20, 21]. The axisymmetric vector nozzle model diagram is shown in Fig. 1.

The expansion blade, convergence blade and the related connecting structure present an axisymmetric distribution therefore a branch containing the expansion blade and convergence blade and connecting structures can also reflect the dynamics of the axisymmetric vector nozzle mechanism to a certain extent effectively. To reduce the complexity of the mechanism and computation burden, one single link branch is selected for dynamic modeling and analysis.

In axisymmetric vector nozzle systems, expansion blade F and convergence blade G are subjected to high-aerodynamic load, which will be transmitted to drag link E. To accurately describe the system's dynamic characteristics, the force transmitting component E is described as a flexible component, and the rest components are described as rigid. The absolute node coordinate formulation is used to describe the flexible component. The radial contact force, tangential friction force, and wear at the clearance joints are calculated by Flores contact force model [40], modified Coulomb friction model [7] and Archard wear law [5], respectively.

The Lagrange equation for the *i* th body of nozzle mechanism system can be expressed as:

$$\frac{d}{dt}\left(\frac{\partial T^i}{\partial \dot{q}^i}\right) - \left(\frac{\partial T^i}{\partial q^i}\right) + \Phi_{q^i}^T \lambda = \frac{1}{2}\int_{V^i} \rho^i \dot{r}^{iT} \dot{r}^i dV^i = \frac{1}{2}\dot{q}^{iT} M^i \dot{q}^i \tag{1}$$

where, $T^i, \phi^T_{q^i}$ and λ are the kinetic energy, the Jacobi matrix and the Lagrange multiplier, respectively. $\rho^i$, $V^i$ and $M^i$ are the density, volume and mass of the *i*th body, respectively.

Considering the constraints imposed on the system, the equation of motion of the multibody system is obtained, as follows:

$$\begin{cases} M\ddot{q} + \Phi^T_q \lambda = Q + F \\ \quad \Phi(q, t) = 0 \end{cases} \tag{2}$$

where $Q$ is the generalised external force, $M$ is the assembled mass matrix, and $F$ is the assembled generalised elastic force. The generalised coordinates and Lagrange multipliers of the equations can be solved using numerical integration such as the Newmark-beta method [27] and HHT-13 [28].

Equation of motion of nozzle mechanism system considering joint clearance, rigid and flexible coupling can be written as:

$$\begin{cases} M_\Sigma \ddot{q} + K\mathrm{q} + \Phi^T_q \lambda = Q_e + F_c \\ \Phi(q, t) = 0 \end{cases} \tag{3}$$

where, $M_\Sigma$ and $K$ are respectively the system mass matrix, damping matrix and stiffness matrix assembled from the individual components. $F_c$ is the generalised contact force, which includes the clearance collision force and friction force. $Q_e$ is the generalised external force. Φ is the constraint equation and $\Phi_q$ is the Jacobi matrix of the constraint equation [29].

Considering that the rigid-flexible coupled system, the mass matrix and generalised coordinates can be written as follows:

$$M_\Sigma = \begin{bmatrix} M_f & 0 \\ 0 & M_r \end{bmatrix}, q = \begin{bmatrix} q_f \\ q_r \end{bmatrix} \tag{4}$$

where, $M_f$ and $M_r$ represent the mass matrices of the flexible and rigid parts, respectively, and $q_f, q_r$ represent the generalised coordinates of the flexible and rigid parts, respectively.

## 3.0  Deep neural network models

DNN is an ML algorithm, which is mainly used to process large-scale complex data, such as images and natural language. DNN can learn highly abstract representations and patterns through multilevel nonlinear transformations.

The structure of DNN includes input, hidden, output layers and all the layers are connected through weights and biases [21]. An effective and reliable dataset is very important for the training of DNN, and the appropriate hyperparameters also significantly affect the performance of DNN, including activation function, loss function, number of hidden layers, number of epochs, number of neurons and optimiser selection.

Activation function is a nonlinear function that is responsible for introducing nonlinear properties to the model, allowing the neural network to learn and represent complex functional relationships [36]. The batch size is the count of training data samples used in performing a single weight update. Due to limitations such as memory, it is generally not recommended to use all available data samples for training at once [34]. Increasing the batch size can reduce the computational cost required for training. The loss function measures the discrepancy between the model's predictions and the actual labels. When training a neural network, the model parameters are optimised by minimising the loss function, allowing the model to make more accurate predictions. Stochastic optimisation methods are used to optimise neural networks [33]. Usually, a small batch of data is obtained, which is treated as stochastic data and gradient descent is performed with this stochastic data [37].

In deep learning, regularisation is used to prevent over fitting by adding constraints and thus improve the robustness of the model [33, 35]. It involves saving and updating the best parameters during training,

stopping when improvements cease and using the last best parameters. This technique limits the optimisation to a smaller parameter space [34, 36]. Early Stopping is chosen as the regularisation method in our DNN model and end the training when the performance of the trained model evaluated through the validation set is no longer increasing.

The selection of appropriate hyperparameters is very important to the performance of the DNN model. We choose the random search method [38] to optimise hyperparameters of the DNN model and finally determine the optimal hyperparameters. Each hidden layer uses the ReLU (Rectified Linear Unit) as activation function, ReLU can prevent the unsaturation of the gradient, which has good results in the application of the multibody dynamics field, and the optimiser is Adam (adaptive moment estimation). It should be mentioned that although AdamW is an improved algorithm based on Adam and L2 regularisation, Adam outperforms AdamW in the DNN model of axisymmetric vector nozzle mechanism. The comparison results will be shown in Section 4. A very large learning rate might prevent convergence to the optimal value, so a learning rate of 0.0001 is chosen, with batch size of 8192. MSE is used as loss function to evaluate the average squared error between the predicted and actual values of the model, respectively. The smaller the value of loss function, the better the performance of the model. As the error decreases, the gradient also decreases, which facilitates convergence even when using a fixed learning rate [22]. The formulas of loss function are given below:

$$\text{MSE} = \frac{1}{N} \sum_{i=1}^{N} \left( y_i - \hat{y}_i \right)^2 \tag{5}$$

where, $N$, $y$, $\hat{y}$ are the number of outputs, baseline values and predicted values in the dataset, respectively.

## 4.0 Numerical results

The DNN model of the axisymmetric vector nozzle is established by limited training data. The adjusted $R^2$, MAE, MSE and RMSE are used as evaluation function to comprehensively evaluate and verify the accuracy of the DNN model. The dynamic response of the DNN at different clearance values was quantified and analysed.

The closer the adjusted $R^2$ value is to 1, the more accurate the prediction results are, and the closer the MAE, MSE and RMSE values are to 0, the more accurate the prediction results are. The formulas for adjusted $R^2$, MAE, MSE and RMSE as shown in the below equations (6)–(9):

$$\textit{Adjusted } R^2 = 1 - \frac{(N-1) \sum_{i=1}^{N} \left( y_i - \hat{y} \right)^2}{(N-p-1) \sum_{i=1}^{N} \left( y_i - \bar{y} \right)^2} \tag{6}$$

$$\text{MAE} = \frac{1}{N} \sum_{i=1}^{N} \left| y_i - \hat{y}_i \right| \tag{7}$$

$$\text{MSE} = \frac{1}{N} \sum_{i=1}^{N} \left( y_i - \hat{y}_i \right)^2 \tag{8}$$

$$\text{RMSE} = \sqrt{\frac{1}{N} \sum_{i=1}^{N} \left( y_i - \hat{y}_i \right)^2} \tag{9}$$

where, $y$, $\hat{y}$, $\bar{y}$ are the baseline value, predicted value and average of the baseline values in the dataset, respectively, N is the number of samples and p is the number of features.

**Table 1.** *Simulation parameters of nozzle mechanism*

| Parameter | Value |
|---|---|
| Pin radius (*m*) | 0.05 |
| Bushing radius (*m*) | 0.0505 |
| Coefficient of wear (*m³/N·m*) | $5.05 \times 10^{-10}$ |
| Friction coefficient | 0.3 |
| Restitution coefficient | 0.9 |
| Young's modulus of the pin material (*GPa*) | 207 |
| Poisson's ratio of the pin material | 0.29 |
| Young's modulus of the bushing material (*GPa*) | 71.7 |
| Poisson's ratio of the bushing material | 0.33 |
| Hardness | 107 |
| Contact length L (*m*) | 0.01 |
| Integration step size (*s*) | 0.125 |

**Table 2.** *Hyperparameters of the DNN for the axisymmetric vector nozzle*

| Hyper-parameters | Choice |
|---|---|
| The number of hidden layers | 9 |
| The number of nodes in each layer | (45, 68, 97, 19, 95, 31,33, 41, 83) |
| Maximum epochs | 180,000 |
| Loss function | MSE |
| Optimiser | Adam |
| Activate the function | ReLU |

### 4.1 Deep neural network model for axisymmetric vector nozzle mechanism

The dynamic equations of axisymmetric vector nozzle mechanism considering joint clearance and rigid-flexible coupling are established and numerically solved, the relevant parameters are shown in Table 1.

The hyperparameters of DNN for the axisymmetric vector nozzle mechanism are summarized in Table 2.

The clearance value of joint in Fig. 1 varies from 0.00 cm to 0.50 cm with a step size of 0.01 cm, and the time varies from 0s to 1s with a step size of 0.125s. The dynamic response of each clearance value is recorded with 800 data points. These data points serve as the training and validation dataset for the neural network. In total, there are 40,800 ($501 \times 800$) data points, with 80% used for training and 20% for testing.

Figure 2 shows the structure of an axisymmetric vector nozzle DNN, including input, hidden and output layers.

Figure 3 shows the angle, angular velocity, displacement, angular acceleration of the expansion blade F and driving force of actuator B under a randomly disrupted test set based on the DNN model.

From the resultant plots of predicted data versus simulated data in Fig. 3, it is clearly shown that the kinematic parameters and driving forces of the axisymmetric vector nozzle remain highly accurate even with randomly test data. It is verified that with appropriate hyperparameters, DNN can predict the dynamic response of the axisymmetric vector nozzle with high accuracy after reasonable training.

In addition, the DNN model of axisymmetric vector nozzles is validated using data outside of the training and test datasets to confirm the robustness of the model that the model maintains a high level of accuracy despite reasonably variation of input parameters, where clearance values from 0.151 cm to 0.159 cm are used as the validation set.
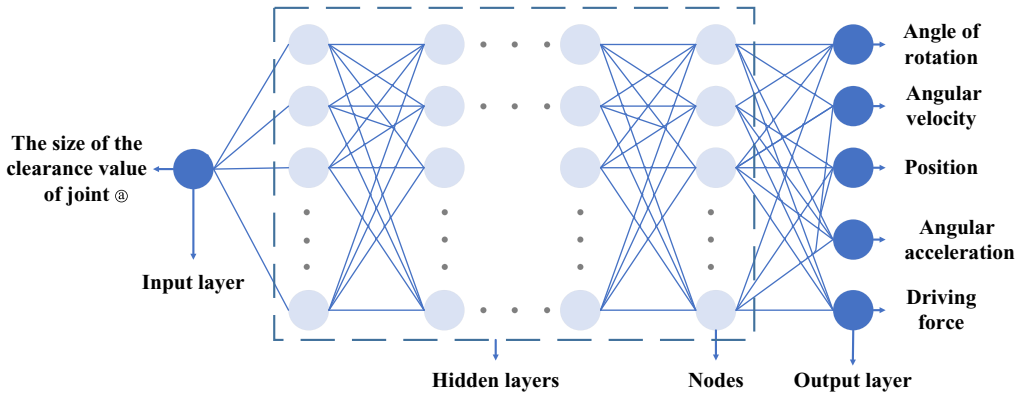
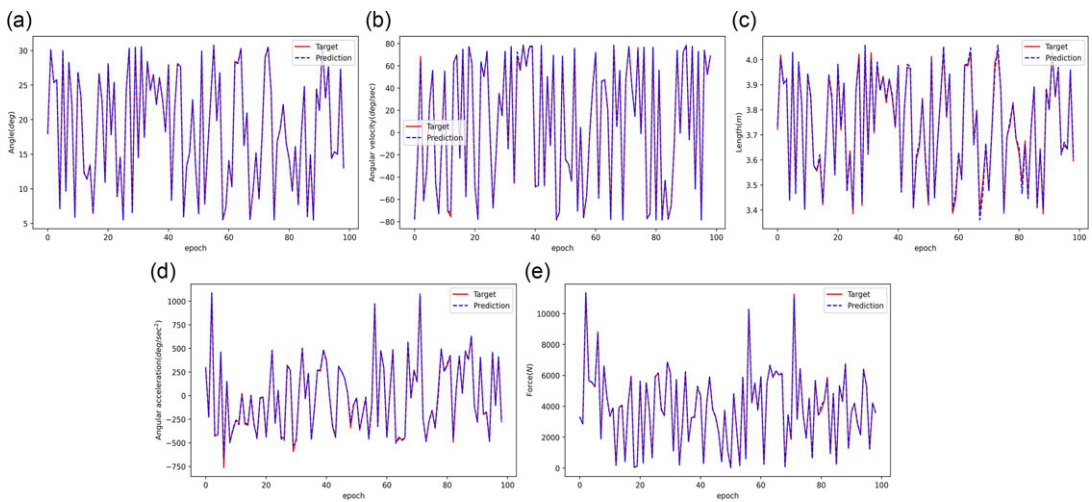*Figure 2.* *Schematic of the DNN for the axisymmetric vector nozzle.*



*Figure 3.* *Representation of the predicted data (blue dashed line) versus simulated data (red solid line) for the axisymmetric vector nozzle DNN model (a) angle of rotation, (b) angular velocity, (c) position, (d) angular acceleration and (e) driving force.*

From Fig. 4, it is indicated that the kinematic parameters and driving forces of the axisymmetric vector nozzle from prediction are coincide with numerical simulation results, which ensures high accuracy even with the validation data set other than the training and test sets. The results show that the DNN model of the axisymmetric vector nozzle can predict the dynamic response of the axisymmetric vector nozzle with high accuracy and robustness. Next, the performance of the DNN model is evaluated by adjusted $R^2$, MAE, MSE and RMSE.

Table 3 shows that the adjusted $R^2$ values of angle, angular velocity, position, angular acceleration and driving force are almost 1. The values of MAE, MSE and RMSE are much smaller compared with the target and predicted values. This indicates that although the presence of joint clearance and flexible deformations in the nozzle system increases the degree of nonlinearity, the neural network model is still able to make high accuracy prediction.

Figure 5 shows the Adjusted $R^2$ of the kinematic parameters and driving force of the DNN of axisymmetric vector nozzle with high accuracy.

**Table 3.** *Adjusted R², MAE, MSE and RMSE values for kinematic parameters of axisymmetric vector nozzles*

| Output features | Adjusted $R^2$ | MAE | MSE | RMSE |
|---|---|---|---|---|
| Angle | 0.9999 | 0.073106 | 0.007524 | 0.0867407415402288 |
| Angular velocity | 0.9994 | 0.664527 | 1.660794 | 1.2887179289859387 |
| Position | 0.9956 | 0.011093 | 0.000217 | 0.0147344265778062 |
| Angular acceleration | 0.9989 | 8.133728 | 150.8366 | 12.281555016687816 |
| Driving force | 0.9997 | 25.09963 | 1532.407 | 39.145979548910894 |
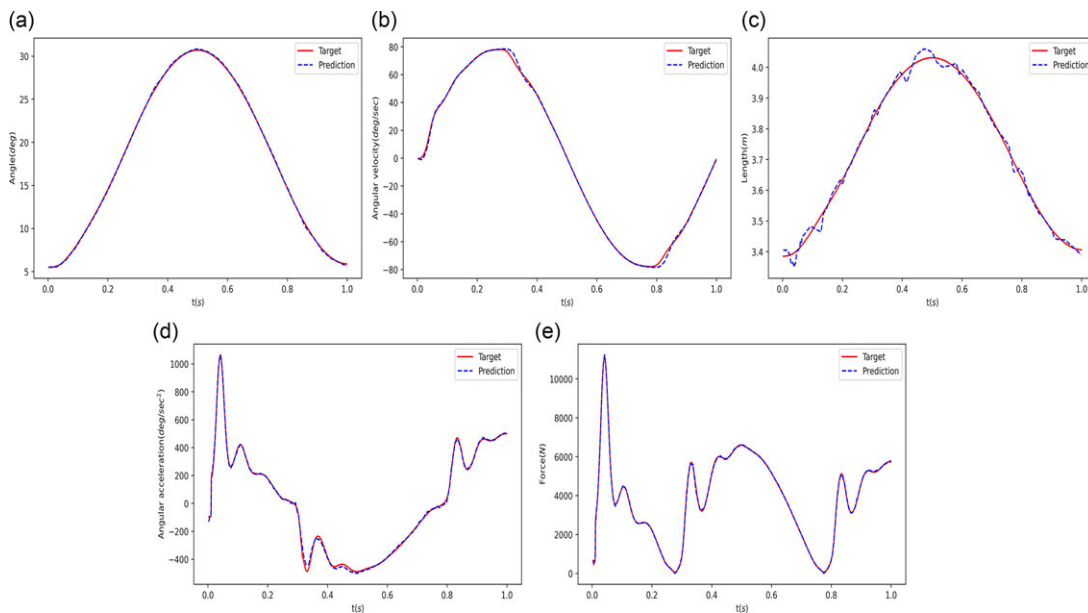


**Figure 4.** *Comparison between the predicted data (blue dashed line) and the simulated data (red solid line) of the axisymmetric vector nozzle expansion blade under the validation set (a) angle of rotation, (b) angular velocity, (c) position, (d) angular acceleration and (e) driving force.*

To investigate the applicability of different optimiser, the DNN model is retrained with AdamW optimiser, while the rest parameters of DNN keep unchanged. Figures 6-8 show the comparison between the test and validation sets with AdamW optimiser. Table 4 shows the values of adjusted R2, MAE, MSE and RMSE with AdamW optimiser. Through comparison of the DNN prediction capability between Adam optimiser and AdamW optimiser shown in Figs 3-8, as well as the adjusted R2, MAE, MSE and RMSE values shown in Table 3 and Table 4, it is clearly reflected that Adam outperforms AdamW.

The DNN model in this paper is trained using GPU (NVIDIA GeForce GTX 1660 TI).

Table 5 shows the time comparison between traditional multibody computation methods and DNN, which may vary according to computer conditions. The time recorded in Table 4 can reflect the computational efficiency of DNN compared with traditional methods.

### 4.2 Dynamics analysis of axisymmetric vector nozzle based on DNN model

Using the trained DNN model, the effect of different clearance values on the dynamic response of the kinematic parameters of the axisymmetric vector nozzle expending blade is analysed.
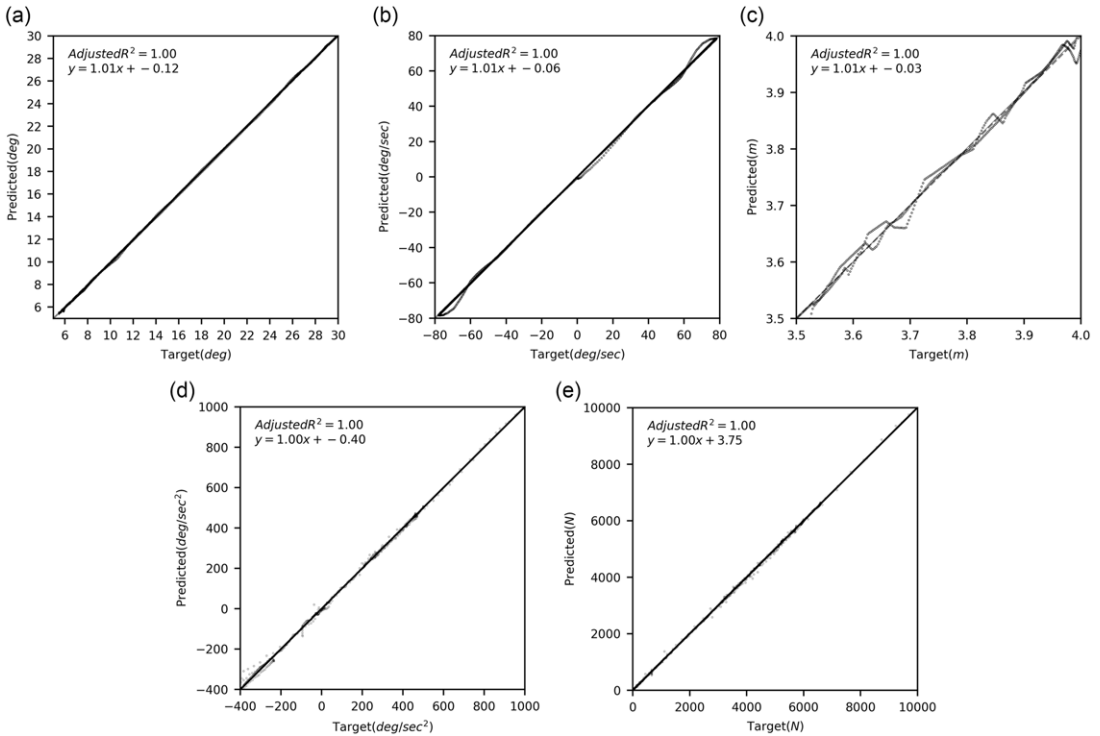
**Figure 5.** *Adjusted R² of the axisymmetric vector nozzle DNN model under the validation set (a) angle of rotation, (b) angular velocity, (c) position, (d) angular acceleration and (e) driving force.*
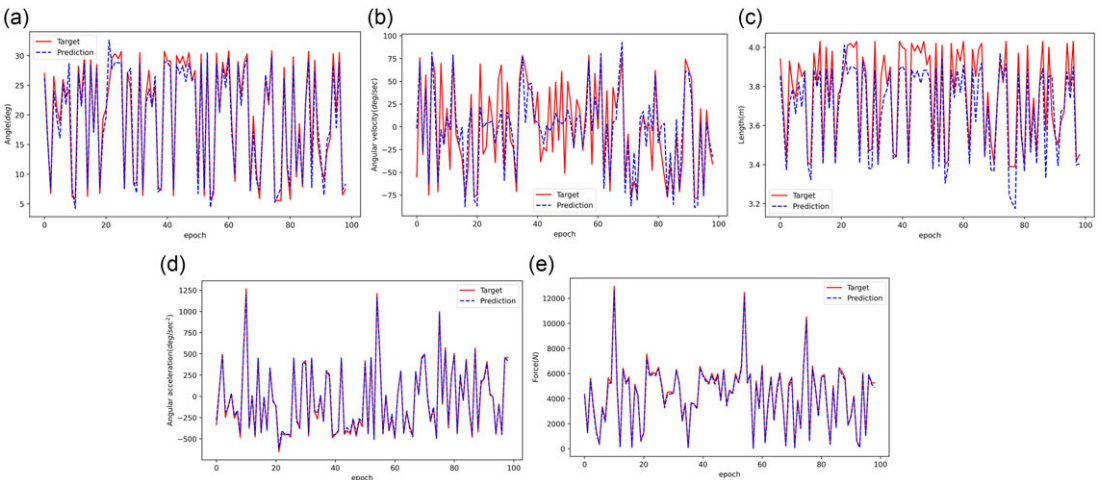


**Figure 6.** *Representation of the predicted data (blue dashed line) versus simulated data (red solid line) for the axisymmetric vector nozzle DNN model with optimiser of AdamW (a) angle of rotation, (b) angular velocity, (c) position, (d) angular acceleration and (e) driving force.*
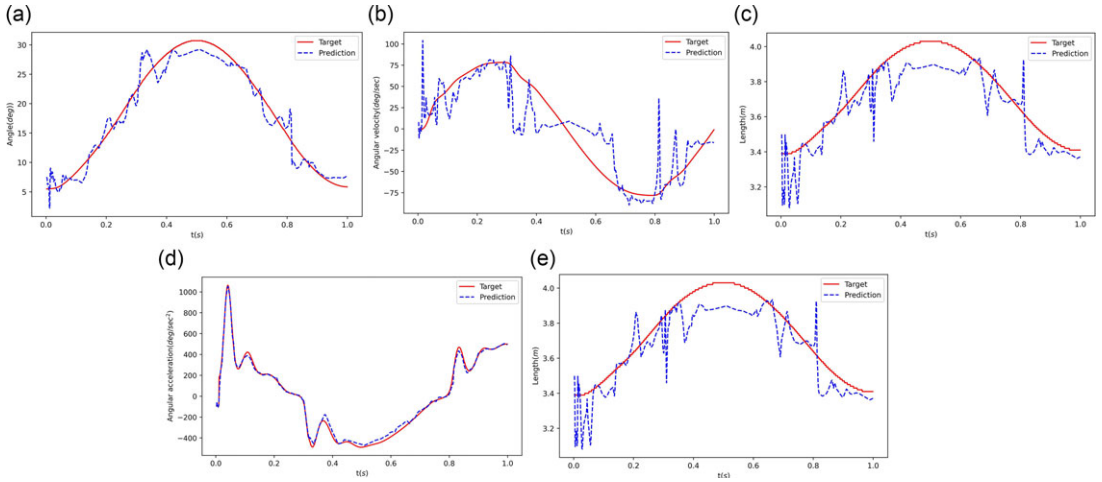
**Figure 7.** *Comparison between the predicted data (blue dashed line) and the simulated data (red solid line) of the axisymmetric vector nozzle expansion blade under the validation set with AdamW optimiser. (a) Angle of rotation, (b) angular velocity, (c) position, (d) angular acceleration and (e) driving force.*



**Figure 8.** *Adjusted $R^2$ of the axisymmetric vector nozzle DNN model under the validation set with AdamW optimiser. (a) Angle of rotation, (b) angular velocity, (c) position, (d) angular acceleration and (e) driving force.*
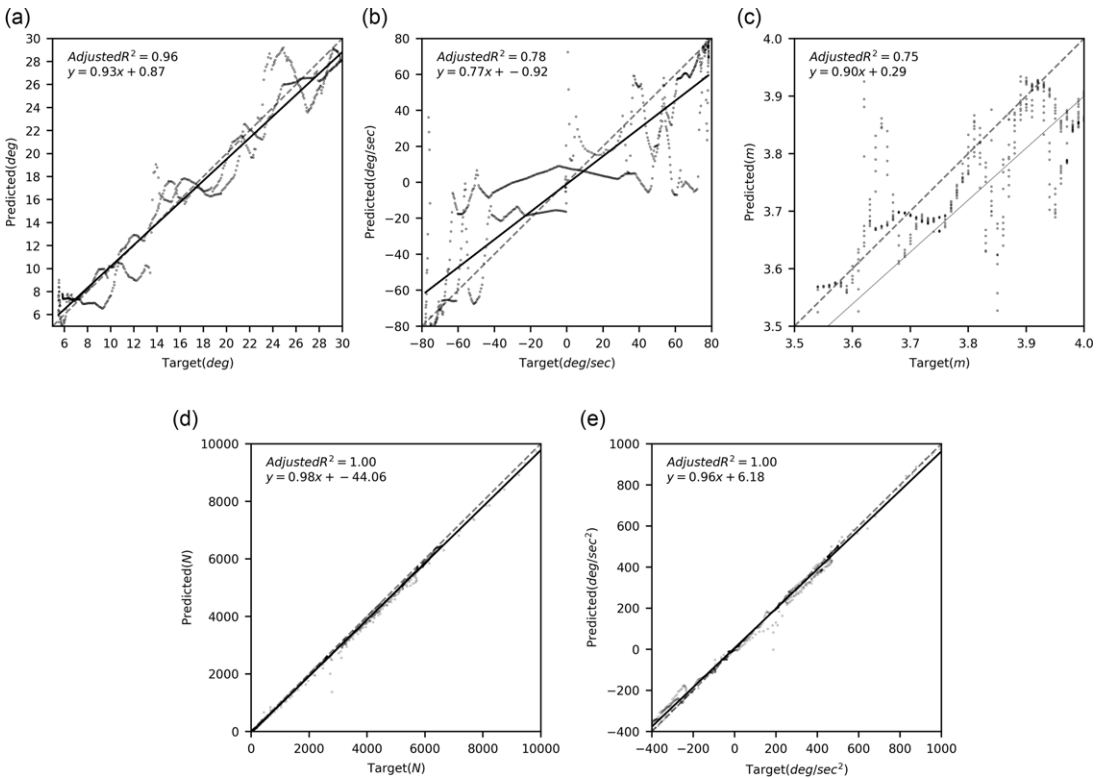
***Table 4.*** *Adjusted $R^2$, MAE, MSE and RMSE values for kinematic parameters of axisymmetric vector nozzles with AdamW optimiser*

| Output features | Adjusted $R^2$ | MAE | MSE | RMSE |
|---|---|---|---|---|
| Angle | 0.9628 | 1.385655 | 2.909238 | 1.7056488794742840 |
| Angular velocity | 0.7797 | 18.33017 | 666.7015 | 25.820563066106462 |
| Position | 0.7511 | 0.088654 | 0.012472 | 0.1116798433167317 |
| Angular acceleration | 0.9952 | 18.37480 | 641.0530 | 25.319025248827830 |
| Driving force | 0.9954 | 115.6763 | 22672.48 | 150.57381780832617 |

***Table 5.*** *Time consuming*

| The training time of DNN | The traditional method calculation time | The prediction time of DNN |
|---|---|---|
| 170,59 s | 867 s | 2.13 ms |

Five different clearance values (0.00cm, 0.10cm, 0.15cm, 0.20cm and 0.25cm, respectively) are chosen to study the effect of clearance on the angle of rotation, angular velocity, position, angular acceleration and driving force of the axisymmetric vector nozzle.

The motion of the axisymmetric vector nozzle is a reciprocal process, 0-0.5s the expansion blade contracts and 0.5-1.0s expansion blade returns to its original position. The dynamic response of the DNN model indicates that the joint clearance has a certain effect on the angle of rotation, angular velocity and position. The influence of clearance on the expansion blade at 0s-0.2s and 0.8s-1.0s is more pronounced compared with 0.2s-0.6s, because the clearance compensates for the changes of the angle and position of the expansion blade to a certain extent, and the variation of angular velocity are caused by the changing of the contact state between the shaft and the bushing due to the clearance. The clearance has a significant effect on the angular acceleration and driving force, especially at the maximum and minimum values, because the clearance causes impacts and collisions between the shaft and the bushing, and leads to the increase of the relative velocity and contact force.

The partial enlargement view in Fig. 9 clearly shows the there is a crossover of the response of different parameters. During the reciprocating movement, the joint clearance leads to a change of contact state between the shaft and the bushing, and results in the opposite effect of the clearance on the parameters of expending blade.

Figure 10 shows the variation of angle, angular velocity, position, angular acceleration and driving force with different clearance values versus no clearance condition, respectively. Overall, larger clearance value results in more pronounced fluctuations of the differential response of the expanding blade. The clearance imposes significant nonlinearity on the dynamic response of the nozzle mechanism. Also with larger clearance value, the peak of the dynamic response appears earlier. With larger clearance, the shaft needs more time to contact with bushing and transmit the movement afterward and also possess higher impact energy due to the longer freely movement time.

From Table 6, it can be seen that the effect of the clearance value on the angular acceleration and driving force of the expansion blade is the most obvious, comes after angle and angular velocity, the impact on position is the minimum. The collision and impact between shaft and bushing due to clearance cause an abrupt change of the contact force, which affects the driving force and angular acceleration significantly.

The results in this section are obtained by the well-trained DNN model of vector nozzle mechanism, although these computational results can also be obtained by the traditional method, it takes more time, as shown in Table 6. Compared with the multibody dynamics simulation by traditional algorithms, DNN can get the prediction results of the mechanism dynamic response in millisecond, and the high accuracy
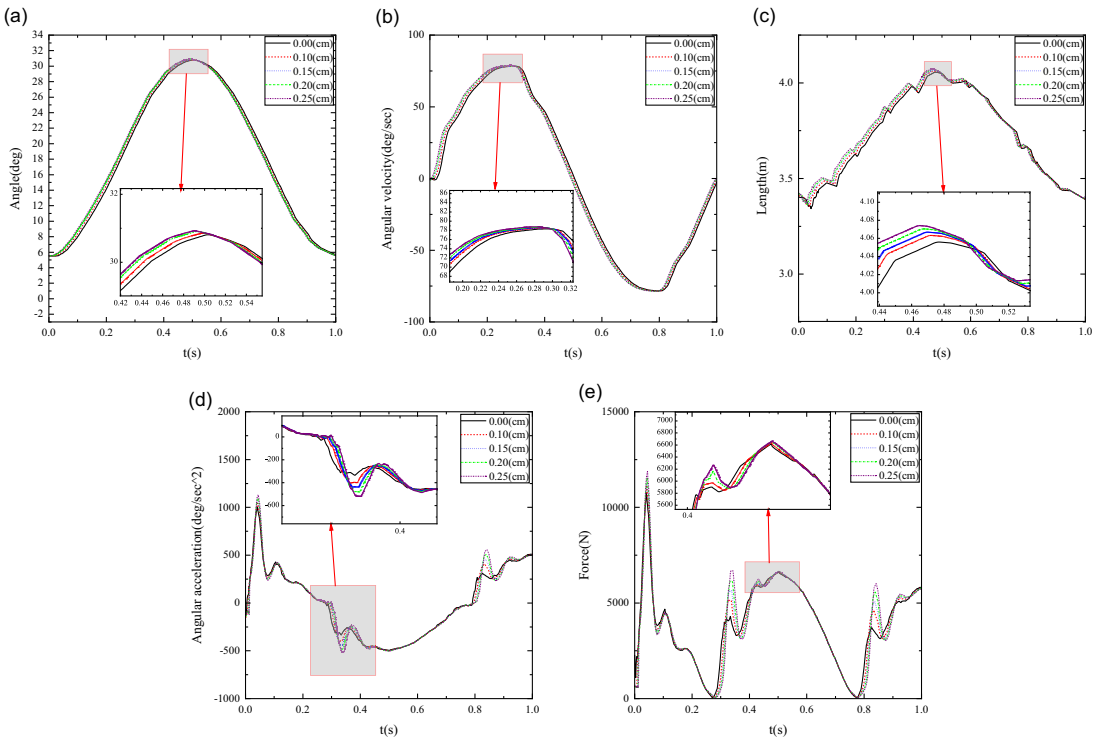
**Figure 9.** *Comparison of dynamic response of axisymmetric vector nozzle expedition blade with different clearance values based on DNN (a) angle of rotation, (b) angular velocity, (c) position, (d) angular acceleration, and (e) driving force.*

of the dynamic response prediction results is guaranteed. Therefore, DNN as an agent model significantly reduces the computational burden associated with traditional multibody dynamics simulation and provides the possibility of real-time monitoring of the dynamic response.

## 5.0 Conclusion

The appropriately trained DNN model of the axisymmetric vector nozzle mechanism shows high accuracy and efficiency in the offline prediction and can be used to make real-time predictions of the dynamic response of the complex axisymmetric vector nozzle system saving huge computation costs. This study analyses the effects of joint clearance on the kinematics and dynamics of the axisymmetric vector nozzle mechanism using a DNN model. It has been demonstrated that joint clearance influences the angular acceleration of the expanding blade and the driving force predominantly, also exerting a significant effect on the angle, angular velocity and position of the expanding blade. The results indicate that an increase in joint clearance value leads to a notable intensification of the fluctuations in the dynamic response of the mechanism, which is due to the increase of the relative velocity and contact force between pin and bushing of the joints. For further analysis of complex axisymmetric vector nozzles mechanism with more variables, training high-precision DNN models require even larger amounts of data and the cost of training DNN models increases significantly. This is the limitation of neural network supervised learning itself, which requires model degradation and data-handling techniques. In addition, the clearance of joints is uncertain quantity essentially due to various external factors such as wear in services environment. It is necessary to study the dynamic response of the mechanism, taking into account the

**Table 6.** *Comparison of the magnitude of change in each parameter of the single link expansion blade of the axisymmetric vector nozzle with different clearance compared to without clearance*

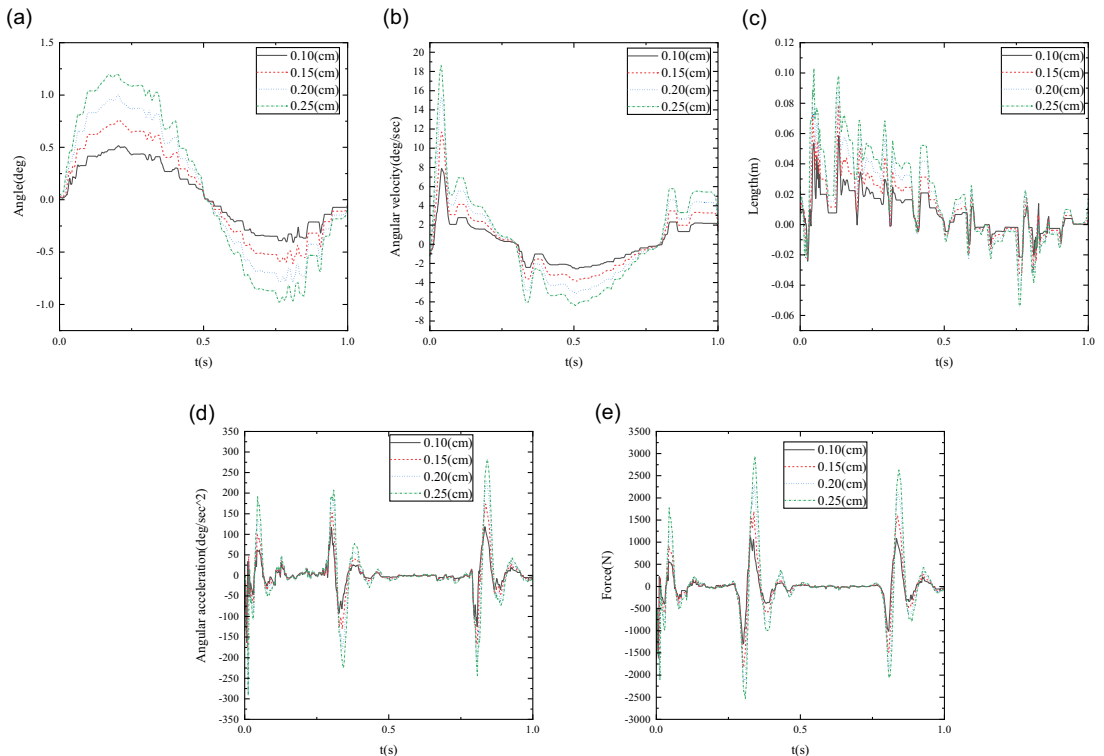| Output features | Max change clearance | Max change value | Max percentage |
|---|---|---|---|
| Angle | 0.25cm | 1.19813deg | 8.60% |
| Angular velocity | 0.25cm | 18.60528deg/sec | 7.51% |
| Position | 0.25cm | 0.10313m | 3.07% |
| Angular acceleration | 0.25cm | 281.7703 deg/sec$^2$ | 102.32% |
| Driving force | 0.25cm | 2941.054N | 78.36% |



**Figure 10.** *Difference of the dynamic response of axisymmetric vector nozzle with different clearance (a) angle of rotation, (b) angular velocity, (c) position, (d) angular acceleration, and (e) driving force.*

uncertainty of the joint clearance. Considering the large samplings during uncertainty analysis, DNN offers new possibilities for the study of joint clearance uncertainty.

**Conflicts of interest.** The authors declare that they have no known competing financial interests or personal relationships that could have appeared to influence the work reported in this paper.

## References

[1] Burcham, Jr, F., Ray, R., Conners, T., & Walsh, K. (1998, July). Propulsion flight research at NASA Dryden from 1967 to 1997. In *34th AIAA/ASME/SAE/ASEE Joint Propulsion Conference and Exhibit* (p. 3712).

[2] Wallace, H., & Bowers, D. (1982). Advanced nozzle integration for air combat fighter application. In *18th Joint Propulsion Conference* (p. 1135).

[3] Koziel, S., Çalık, N., Mahouti, P., & Belen, M.A. (2021). Accurate modeling of antenna structures by means of domain confinement and pyramidal deep neural networks. *IEEE Transactions on Antennas and Propagation*, **70**(3), 2174–2188.

[4] Nguyen, L., & Gilert, W. (1990, May). Impact of emerging technologies on future combat aircraft agility. In *Orbital Debris Conference: Technical Issues andFuture Directions* (p. 1304).

[5] Rajesh, A.M., Doddamani, S., K,M.K., & Bharath, K.N. (2020). Dry sliding wear simulation of hybrid aluminum metal matrix composites. *Advanced Composites and Hybrid Materials*, **3**, 120-126.

[6] Kirkwood, C., Economou, T., Pugeault, N., & Odbert, H. (2022). Bayesian deep learning for spatial interpolation in the presence of auxiliary information. *Mathematical Geosciences*, **54**(3), 507–531.

[7] Flamm, J., Deere, K., Mason, M., Berrier, B., & Johnson, S. (2007, July). Experimental study of an axisymmetric dual throat fluidic thrust vectoring nozzle for supersonic aircraft application. In *43rd AIAA/ASME/SAE/ASEE Joint Propulsion Conference & Exhibit* (p. 5084).

[8] Counts, B. (2016). It's Time to Cut Our Losses on the F-35. International Policy *Digest*, **3**(8).

[9] Miao, H., Li, B., Liu, J., He, A., & Zhu, S.. (2019). Effects of revolute clearance joint on the dynamic behavior of a planar space arm system. Proceedings of the Institution of Mechanical Engineers, **233**(5), 1629–1644.

[10] Xiulong, C., Yonghao, J., Yu, D., & Qing, W.. (2018). Dynamics behavior analysis of parallel mechanism with joint clearance and flexible links. *Shock and Vibration*, **2018**(PT.2), 1–17.

[11] Li, Y., Wu, J., Tedrake, R., Tenenbaum, J.B., & Torralba, A. (2018). Learning particle dynamics for manipulating rigid bodies, deformable objects, and fluids. arxiv preprint arxiv:1810.01566.

[12] Go, M.S., Han, S., Lim, J.H., & Kim, J.G. (2024). An efficient fixed-time increment-based data-driven simulation for general multibody dynamics using deep neural networks. *Engineering with Computers*, **40**(1), 323–341.

[13] Yu-Tong, L., & Yu-**n, W. (2019, August). Singularities in Axisymmetric Vectoring Exhaust Nozzle and a Feasible Singularity-Free Approach. In *International Design Engineering Technical Conferences and Computers and Information in Engineering Conference* (Vol. 59261, p. V006T09A015). American Society of Mechanical Engineers.

[14] Ansari, H., Tupy, M., Datar, M., & Negrut, D. (2010). Construction and use of surrogate models for the dynamic analysis of multibody systems. *SAE International Journal of Passenger Cars-Mechanical Systems*, **3**(2010-01-0032), 8–20.

[15] Geman, A., Geman, D., Graffigne, C., & Dong, P. (1984). IEEE Transactions on Pattern Analysis and Machine Intelligence.

[16] Kraft, S., Causse, J., & Aurélie Martinez. (2019). Black-box modelling of nonlinear railway vehicle dynamics for track geometry assessment using neural networks. Informa UK Limited(9).

[17] Jian, W., Xiaochuan, M.A., Jiayin, C., Jingmang, X.U., & Ping, W.. (2017). Study of matching performance of chn60n rail with different wheel treads in high-speed railway. Journal of the China Railway Society.

[18] Kurvinen, E., Suninen, I., Orzechowski, G., Choi, J.H., Kim, J.G., & Mikkola, A. (2021). Accelerating design processes using data-driven models. In *Real-time Simulation for Sustainable Production* (pp. 65–76). Routledge.

[19] Byravan, A., & Fox, D. (2017). *Se3-nets: learning rigid body motion using deep neural networks*. IEEE.

[20] Choi, H.S., An, J., Han, S., Kim, J.G., Jung, J.Y., & Choi, J., et al. (2021). Data-driven simulation for general-purpose multibody dynamics using deep neural networks. Springer Netherlands(4).

[21] Choi, H.S., An, J., Kim, J.G., Jung, J.Y., & Choi, J.H.. (2019). Data-driven simulation for general purpose multibody dynamics using deep neural networks.

[22] Bernal, E., J.Orús, J.M.Rodríguez-Fortún, Nadal, I., & Putz, T.. (2011). Use of co-simulation and model order reduction techniques in automotive industry: Application to an electric park brake (EPB). EAEC European automotive congress. Area of Research, Development & Technological Services, Instituto Tecnológico de Aragón (ITA), 7-8 María de Luna, 50018 Zaragoza, Spain;Area of Research, Development & Technological Services, Instituto Tecnológico de Aragón (ITA), 7-8 María de Luna, 50018.

[23] Ting, J.A., Mistry, M., Peters, J., Schaal, S., & Nakanishi, J.. (2006). A Bayesian Approach to Nonlinear Parameter Identification for Rigid Body Dynamics. Robotics: Science and Systems II, August 16-19, 2006. University of Pennsylvania, Philadelphia, Pennsylvania, USA. DBLP.

[24] Kim, J.H., & Joo, C.B.. (2014). Numerical construction of balanced state manifold for single-support legged mechanism in sagittal plane. *Multibody System Dynamics*, **31**(3), 257–281.

[25] Yunguang, Y., Shi, D., Krause, P., & Hecht, M.. (2019). A data-driven method for estimating wheel flat length. Vehicle System Dynamics.

[26] Ye, Y.G., Shi, D.C., Poveda-Reyes, S., & Hecht, M. (2020). Erratum to: Quantification of the influence of rolling stock failures on track deterioration. *Journal of Zhejiang University-SCIENCE A*, **21**, 938–938.

[27] Newmark, N.M.. (1959). A method of computation for structural dynamics. *Proc Asce*, **85**(1), 67–94.

[28] Negrut, D., Rampalli, R., Ottarsson, G., & Sajdak, A.. (2007). On an implementation of the hilber-hughes-taylor method in the context of index 3 differential-algebraic equations of multibody dynamics (detc2005-85096). *Journal of Computational & Nonlinear Dynamics*, **2**(1), 73–85.

[29] Li, Y., Wang, C., & Huang, W. (2019). Rigid-flexible-thermal analysis of planar composite solar array with clearance joint considering torsional spring, latch mechanism and attitude controller. Nonlinear Dynamics.

[30] Zhang, H., Wu, Q., Zeng, H., Meng, L., Luo, Z., & Han, Q. (2024). Analysis of the dynamic of vector nozzle adjustment mechanism considering the effect of joint clearance. *Journal of Vibration Engineering & Technologies*, **12**(4), 6137–6154.

[31] Changpeng, C.A.I., Yerong, P.E.N.G., Zheng, Q., & Zhang, H. (2022). Vector deflection stability control of aero-engine based on linear active disturbance rejection. *Chinese Journal of Aeronautics*, **35**(8), 221–235.

[32] Du, Q., Li, J., **e, L., Fu, X., & Wang, Y. (2022, September). Research on Reliability Analysis of Axial-Symmetric Vectoring Exhaust Nozzle Based on Parametric Modeling. In *Journal of Physics: Conference Series* (Vol. 2338, No. 1, p. 012061). IOP Publishing.

[33] Zheng, Q., Zhao, P., Zhang, D., & Wang, H.. (2021). Mr-dcae: manifold regularization-based deep convolutional autoencoder for unauthorized broadcasting identification. International Journal of Intelligent Systems.

[34] Zheng, Q., Zhao, P., Wang, H., Elhanashi, A., & Saponara, S. (2022). Fine-grained modulation classification using multi-scale radio transformer with dual-channel representation. *IEEE Communications Letters*, **26**(6), 1298–1302.

[35] Zheng, Q., Tian, X., Yu, Z., Wang, H., Elhanashi, A., & Saponara, S. (2023). DL-PR: Generalized automatic modulation classification method based on deep learning with priori regularization. *Engineering Applications of Artificial Intelligence*, **122**, 106082.

[36] Zheng, Q., Saponara, S., Tian, X., Yu, Z., Elhanashi, A., & Yu, R. (2024). A real-time constellation image classification method of wireless communication signals based on the lightweight network MobileViT. *Cognitive Neurodynamics*, **18**(2), 659–671.

[37] Zheng, Q., Tian, X., Yu, Z., Ding, Y., Elhanashi, A., Saponara, S., & Kpalma, K. (2023). MobileRaT: A Lightweight Radio Transformer Method for Automatic Modulation Classification in Drone Communication Systems. *Drones*, **7**(10), 596.

[38] He, X., Zhao, K., & Chu, X. (2021). AutoML: A survey of the state-of-the-art. *Knowledge-based systems*, **212**, 106622.

[39] Deng, R., Kong, F., & Kim, H.D. (2014). Numerical simulation of fluidic thrust vectoring in an axisymmetric supersonic nozzle. *Journal of Mechanical Science and Technology*, **28**, 4979–4987.

[40] Hedrih, K.R.S.. (2019). Vibro-impact dynamics of two rolling heavy thin disks along rotate curvilinear line and energy analysis. *Nonlinear Dynamics*, **98**(4), 2551–2579.